



AIAA-90-0221

APPLICATION OF DYNAMICAL SYSTEMS
THEORY TO THE HIGH ANGLE OF
ATTACK DYNAMICS OF THE F-14

C. Jahnke and F. Culick

California Institute of Technology

Pasadena, CA 91125

28th Aerospace Sciences Meeting

January 8-11, 1990/Reno, Nevada

APPLICATION OF DYNAMICAL SYSTEMS THEORY
TO THE HIGH ANGLE OF ATTACK DYNAMICS OF THE F-14

Craig C. Jahnke* and Fred E. C. Culick**

California Institute of Technology

Pasadena, CA 91125

ABSTRACT

Dynamical systems theory has been used to study the nonlinear dynamics of the F-14. An eight degree of freedom model that does not include the control system present in operational F-14's has been analyzed. The aerodynamic model, supplied by NASA, includes nonlinearities as functions of the angles of attack and sideslip, the rotation rate, and the elevator deflection. A continuation method has been used to calculate the steady states of the F-14 as continuous functions of the control surface deflections. Bifurcations of these steady states have been used to predict the onset of wing rock, spiral divergence, and jump phenomena which cause the aircraft to enter a spin. A simple feedback control system was designed to eliminate the wing rock and spiral divergence instabilities. The predictions were verified with numerical simulations.

LIST OF SYMBOLS

α - angle of attack
 b - wing span
 β - angle of sideslip
 c - wing chord
 δa - aileron deflection
 δe - elevator deflection
 δr - rudder deflection
 g - gravity
 I_x - inertia about aircraft x -axis
 I_y - inertia about aircraft y -axis
 I_z - inertia about aircraft z -axis
 ℓ - roll moment
 m - pitch moment
 n - yaw moment

Ω - rotation rate about the velocity vector
 $\hat{\Omega}$ - nondimensional rotation rate about the velocity vector ($= \frac{b}{2V} \Omega$)
 ϕ - roll angle
 ψ - yaw angle
 p - roll rate
 q - pitch rate
 Q - dynamic pressure
 r - yaw rate
 S - wing surface area
 T - applied thrust
 θ - pitch angle
 V - aircraft speed
 W - aircraft weight
 X - aerodynamic force along aircraft x -axis
 Y - aerodynamic force along aircraft y -axis
 Z - aerodynamic force along aircraft z -axis

I. INTRODUCTION

Nonlinear dynamics are central to several important aircraft motions, including roll-coupling and stall/spin phenomena. Roll-coupling involves nonlinearities which result from inertial coupling and stall/spin phenomena involve both nonlinear aerodynamics and inertial coupling. Analysis of these phenomena is difficult because linearized equations of motion cannot be used. Indeed, roll-coupling instabilities were first discovered in flight, often with fatal results, because the linearized equations of motion used for analysis at the time did not contain the instability.

William Phillips' [1948] first analyzed the roll-coupling problem by treating the roll rate as a parameter in the linearized pitching and yawing moment equations. His analysis showed that aircraft with low inertia in roll could experience instabilities in pitch or yaw for certain critical roll rates. Inertial coupling also results in large sideslip deviations which cause high loads on the vertical tail.

* Member AIAA

** Professor of Jet Propulsion and Mechanical Engineering, Fellow AIAA

Copyright ©1990 by Craig C. Jahnke. Published by the American Institute of Aeronautics and Astronautics, Inc. with permission.

Much of the subsequent research was devoted to predicting the maximum tail loads during maneuvers involving roll-coupling. The typical method of analysis was to run large number of numerical simulations using simplified equations of motion but retaining nonlinearities which are important to roll-coupling phenomena. Gates and Minka [1959] calculated the steady states of the simplified equations of motion for an aircraft and showed that the jump phenomena associated with roll-coupling instabilities resulted in the aircraft jumping from one steady state to another.

Subsequent researchers expanded the techniques used by Gates and Minka to analyze more complete aerodynamic models. Young, Schy, and Johnson [1980] developed an iterative technique for determining the steady states of the fifth order equations of motion which included an aerodynamic model that was a nonlinear function of the angle of attack. Their results clearly show the benefits of calculating the steady states of the equations of motion for an aircraft. The global nature of the results provides a qualitative understanding of the dynamics of the aircraft and in many cases, the result of a jump in the state of the aircraft caused by a roll-coupling instability could be predicted with the knowledge of the steady states of the aircraft.

Analysis of stall/spin phenomena developed along the same general pattern as analysis of the roll-coupling instability. Initially most work involved numerical simulations of spin entry and attempts to determine recovery techniques. Early simulations of spin entry and recovery compared poorly with spin tunnel and flight tests. The reason for the disparities between the numerical simulations and flight tests was discovered by Chambers, Bowman, and Anglin [1969] who showed that rotary balance data were necessary to correctly model the aerodynamics during a spin.

More recently, analysis of stall/spin phenomena has involved attempts to determine the steady spin modes of aircraft. Adams [1972] developed an iterative search technique for determining steady state spins. His results compared poorly with flight tests because he did not include rotary balance data in his aerodynamic models. Tischler and Barlow [1981] developed a graphical technique for determining the steady spins of several general aviation aircraft. Rotary balance data was included in the aerodynamic model and they obtained fairly good comparisons with flight tests.

A major short coming of the techniques mentioned above is that they require some type of simplification of the equations of motion and/or the aerodynamic models. Continuation methods are numerical techniques for calculating the steady states of systems of ordinary differential equations and have recently been used to study roll-coupling and high angle of attack instabilities. Guicheteau [1981] and Planeaux [1988] used continuation methods to analyze high angle of attack instabilities of jet fighters and Jahnke and Culick [1988] used continuation methods to analyze the roll-coupling behavior of a jet fighter.

In this work we use a continuation method to determine the steady states of the F-14 as functions of the aileron and elevator deflections. Bifurcations of these steady states are determined and results from dynamical systems theory are used to predict the response of the aircraft after a bifurcation is encountered. Numerical simulations are used to verify the predictions. Instabilities during longitudinal maneuvers were shown to cause wing rock and spiral divergence and instabilities during lateral maneuvers were shown to cause the F-14 to enter spins. Steady spins were determined as functions of the aileron and elevator deflections. Attempts to recover from developed spins proved unsuccessful.

THEORETICAL BACKGROUND

2.1 Dynamical Systems Theory

Dynamical systems theory is a methodology for studying systems of ordinary differential equations. Many systems have been studied using dynamical systems theory but it has not been widely used to study the equations of motion for an aircraft. The important ideas of dynamical systems theory used in this report will be introduced in the following paragraphs. More information on dynamical systems theory can be found in the book of Guckenheimer and Holmes [1983].

The first step in analyzing a system of nonlinear differential equations, in the dynamical systems theory approach, is to calculate the steady states of the system and their stability. Steady states can be found by setting all time derivatives equal to zero and solving the resulting set of algebraic equations. The Hartman-Grobman Theorem [Guckenheimer and Holmes, Chapter 1, page 13] proves that the local stability of a steady state can be determined by linearizing the equations of motion about the steady state and calculating the eigenvalues. A

steady state is stable if the real part of all eigenvalues are negative. The state of the system will be attracted to stable steady states and repelled from unstable steady states.

The Implicit Function Theorem [Ioos and Joseph, Chapter 2, pages 13-14.] proves that the steady states of a system are continuous functions of the parameters of the system. Thus, the steady states of the equations of motion for an aircraft are continuous functions of the control surface deflections. Stability changes can occur as the parameters of the system are varied in such a way that the real parts of one or more eigenvalues of the linearized system change sign. Changes in the stability of a steady state lead to qualitatively different responses for the system and are called bifurcations. Stability boundaries can be determined by searching for steady states which have one or more eigenvalues with zero real parts.

There are many types of bifurcations and each type has a different effect on the response of the system. Qualitative changes in the response of the system can be predicted by determining how many and what type of eigenvalues have zero real parts at the bifurcation point. Bifurcations for which one real eigenvalue is zero lead to the creation or destruction of two or more steady states. Bifurcations for which one pair of imaginary eigenvalues has zero real parts can lead to the creation or destruction of periodic motions. Bifurcations for which more than one real eigenvalue or more than one pair of complex eigenvalues has zero real parts lead to very complicated behavior and are beyond the scope of this report. Three types of bifurcations were found to occur in the steady states of the F-14: saddle-node, pitchfork and Hopf. Appendix A contains simple examples of each of these bifurcations and brief discussions of the effects they have on the response of the system.

2.2 Continuation Methods

Continuation methods are a direct result the Implicit Function Theorem, which proves that the steady states of a system are continuous functions of the parameters of the system. The general technique is to fix all parameters but one and trace the steady states of the system as a function of this parameter. If one steady state of the system is known, a new steady state can be approximated by linear extrapolation from the known steady state (see Figure 1). The slope of the curve at the steady state can be determined by taking the derivative of the

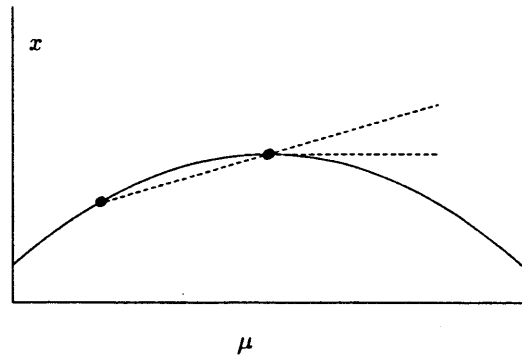


Figure 1: Graphical representation of continuation method.

equation given by setting all time derivatives equal to zero.

If two steady states are known, a new steady state can be approximated by linear extrapolation through the known steady states as shown in Figure 1. This technique is much more efficient than calculating the exact slope at the known steady state, which requires a matrix inversion. Errors between the approximate steady state and the true steady state can be reduced with Newton's method. The stability of each steady state can be determined and any changes in stability will signify a bifurcation. There are several continuation method algorithms, in this work we use the algorithm developed by Doedel and Kernevez [1985] which is based on the work of Keller [1977].

III. MODEL OF AIRCRAFT DYNAMICS

The purpose of this work has been to use dynamical systems theory to analyze the equations of motion for an aircraft. This work concentrated on the high angle of attack dynamics of the F-14 for several reasons. The main reason is that high angle of attack dynamics are inherently nonlinear and cannot be analyzed by the traditional linear techniques. Also, with the recent emphasis on developing fighters that can maneuver at high angles of attack it was felt that results on high angle of attack flight would be particularly relevant.

The equations of motion used in this study assumed a rigid aircraft, no applied thrust, and constant atmospheric density. The equations were written in the principal axis system and consist of:

- rotational equations

$$\dot{p} = \frac{I_y - I_x}{I_x} qr + \frac{1}{I_x} \ell$$

$$\dot{q} = \frac{I_x - I_y}{I_y} pr + \frac{1}{I_y} m$$

$$\dot{r} = \frac{I_x - I_y}{I_x} pq + \frac{1}{I_x} n$$

- translational equations

$$\dot{\alpha} = q - (p \cos \alpha + r \sin \alpha) \tan \beta + \frac{1}{MV \cos \beta} (Z \cos \alpha - X \sin \alpha) + \frac{g}{MV \cos \beta} (\sin \alpha \sin \theta + \cos \alpha \cos \theta \cos \phi)$$

$$\dot{\beta} = p \sin \alpha - r \cos \alpha + \frac{1}{MV} (Y \cos \beta - (X \cos \alpha + Z \sin \alpha) \sin \beta) + \frac{g}{V} (\cos \alpha \sin \beta \sin \theta + \cos \beta \cos \theta \sin \phi - \sin \alpha \sin \beta \cos \theta \cos \phi)$$

$$\dot{V} = \frac{1}{M} (X \cos \alpha + Z \sin \alpha) \cos \beta + Y \sin \beta + g (\sin \beta \cos \theta \sin \phi - \cos \alpha \cos \beta \sin \theta + \sin \alpha \cos \beta \cos \theta \cos \phi)$$

- Euler angles

$$\dot{\theta} = q \cos \phi - r \sin \phi$$

$$\dot{\phi} = p + (q \sin \phi + r \cos \phi) \tan \theta$$

$$\dot{\psi} = (q \sin \phi + r \cos \phi) \sec \theta$$

The equation for the yaw angle, ψ , is decoupled from the other equations, so the system can be reduced from a ninth to an eighth order system.

The aerodynamic model used in this work was supplied by NASA Ames Dryden Flight Research Center and is the aerodynamic model used in their flight simulators. The model includes nonlinearities as functions of the angles of attack and sideslip, the rotation rate, and the elevator deflection. Data was reported for angles of attack from zero to 90 degrees, angles of sideslip from negative 20 to positive 20 degrees, nondimensional rotation rates, $\bar{\Omega}$, from negative 0.54 to positive 0.54, and elevator deflections from negative 30 to positive 10 degrees. Mach number effects were included in the model provided by NASA but were not used in this work. This limited the Mach number of the results presented here to be less than 0.60.

The aerodynamic model has the form:

$$C_\ell = C_\ell(\alpha, \beta, \bar{\Omega}, \delta e)$$

$$C_m = C_m(\alpha, \beta, \bar{\Omega}, \delta e)$$

$$C_n = C_n(\alpha, \beta, \bar{\Omega}, \delta e)$$

$$C_X = C_X(\alpha, \beta, \delta e)$$

$$C_Y = C_Y(\alpha, \beta, \bar{\Omega}, \delta e)$$

$$C_Z = C_Z(\alpha, \beta, \bar{\Omega}, \delta e)$$

where the nondimensional rotation rate about the velocity vector is defined as

$$\bar{\Omega} = \frac{b}{2V} ((p \cos \alpha + r \sin \alpha) \cos \beta + q \sin \beta).$$

One important quality of this aerodynamic model is that the rudder is ineffective for angles of attack greater than 55 degrees. This will be significant when attempting to develop spin recovery techniques.

A continuous first derivative was required for the continuation method algorithm to converge so the data were approximated with bicubic functions using an algorithm of Press, Flannery, Teukolsky, and Vetterling [1988]. This type of fit introduces large curvatures to the aerodynamic data. The data were approximated with linear interpolation in the simulations to make sure the bifurcations reported by the continuation method were not a result of the curvatures introduced by the data fit.

RESULTS

We have studied the dynamics of the F-14 by determining the steady states of the equations of motion and seeking bifurcations. The steady states are plotted as functions of the aileron and elevator deflections. Atmospheric density is 0.53 kg/m^3 , which corresponds to an altitude of 20,000 feet and the applied thrust is zero for the results presented here. Including nonzero applied thrust in the analysis would change the steady state velocity of the aircraft, but not the qualitative nature of the results. Jahnke [1990] has shown that for subsonic speeds, both high angle of attack and roll-coupling instabilities are insensitive to airspeed. Also, since the aerodynamic model used in this study was limited to Mach numbers below 0.60, a wider range of control surface deflections could be analyzed when zero applied thrust was used in the analysis. The small canards included on operational F-14's to provide longitudinal stability are not included in the aircraft model used in this study. Also, the spoilers are retracted and the wings fully forward for the results presented here.

4.1 Longitudinal Maneuvers

Figure 2 shows the steady states of the F-14 which are at low angles of attack. Steady states represented by curve 1 are the longitudinal trim conditions and the steady states represented by curves 2N and 2P represent spirally divergent motions. The 'N' and 'P' are used to denote steady states

with negative and positive roll rates respectively. Figure 2 shows that for elevator deflections greater than negative 7 degrees the trim conditions of the F-14 are stable. The steady states represented by curve 1 were calculated up to an elevator deflection of negative 40 degrees. A smaller range is shown in Figure 2 so that the instabilities which occur for small elevator deflections can be clearly seen. The trim condition for a given elevator deflection can be determined by drawing a vertical line representing the desired elevator deflection on each plot; each intersection of this line with the curve of steady states gives a possible steady state of the aircraft.

For elevator deflections between negative 6.7 and negative 5.4 degrees the steady state trim conditions of the F-14 are unstable as a result of two Hopf bifurcations. Hopf bifurcations can lead to periodic motions, so it is possible that for elevator deflections between negative 6.7 and negative 5.4 degrees the F-14 will undergo periodic motions. Figure 3 shows a simulation in which the elevator deflection is changed from negative 5 degrees to negative 6 degrees, putting the aircraft in the region of unstable steady states. The figure shows that a slowly developing wing rock is present for an elevator deflection of negative 6 degrees. The oscillations grow very slowly and have a period of about four seconds, so they would not be a danger to pilots. Note that the magnitude and frequency of these oscillations could change if the airspeed were increased (by applying thrust) or the atmospheric density changed (due to changing the altitude).

For elevator deflections between negative 3 and negative 4 degrees there are three possible steady states for the aircraft. The trim conditions (curve 1) are unstable while the two steady states representing spiral divergence are steady. Thus, for elevator deflections between negative 3 and negative 4 degrees the F-14 would experience spiral divergence. A simulation of this is shown in Figure 4. The roll angle of the aircraft changes rapidly in response to a one-tenth of a degree aileron perturbation and then continues to slowly increase. The pitch angle and velocity also change as the aircraft goes into a shallow spiral. This motion grows very slowly and could easily be controlled by a pilot.

These instabilities could also be controlled with a simple feedback control system. Wing rock can be a result of low damping in roll [Ericsson, 1988], and spiral divergence can be a result of insufficient dihedral effect [Nelson, 1989]. Feedback to the ailerons can be used to supplement both of these stability

derivatives. Roll rate feedback can be used to increase the effective roll damping and sideslip feedback can be used to supplement the dihedral effect. Figure 5 shows the steady states which are at low angles of attack when sideslip and roll rate feedback to the aileron is included in the aircraft model. The figure shows that both regions of instability, wing rock and spiral divergence, have been eliminated through the use of feedback to the ailerons. It should be noted that the effect of the control system was computed on the steady states of the nonlinear equations of motion. With continuation methods it is possible to compute the effect of feedback on nonlinear systems.

4.2 Lateral Maneuvers

Figure 6 shows the steady states of the F-14 as a function of aileron deflection for an elevator deflection of negative 10 degrees and no rudder deflection. Several differences are evident between this figure and Figure 4.2 which showed the longitudinal steady states of the aircraft. The most obvious difference is that multiple steady states exist for most aileron deflections. For example a vertical line representing zero degrees of aileron deflection intersects five steady states. Three of these steady states are stable so the aircraft could exhibit one of three steady states for zero aileron deflection.

One stable steady state at zero aileron deflection represents the trim condition for an elevator deflection of negative 10 degrees (i.e. $p = q = r = \beta = \phi = 0$). The other two stable steady states represent spins. This can be seen by noting that these steady states have angles of attack near 80 degrees and large steady state yaw rates. The segment of stable steady states containing the trim condition for an elevator deflection of negative 10 degrees only exists for aileron deflections between negative 12 and positive 12 degrees because of the two saddle-node bifurcations that occur at these aileron deflections.

For example, see the steady state angles of attack shown in Figure 6. If the aircraft is trimmed at an elevator deflection of negative 10 degrees the steady state angle of attack will be given by the angle of attack at zero aileron deflection contained in the curve of stable low angle of attack steady states. If the aileron deflection is increased slowly enough, the steady state of the aircraft will be given by the curve of stable low angle of attack steady states up to an aileron deflection of 12 degrees. For aileron deflections greater than 12 degrees, the steady which are at low angles of attack do not exist so the aircraft will jump to a new stable motion. This new

motion could be either a new stable steady state or some type of stable time dependent motion.

Figure 7 shows a simulation of the maneuver described above. The simulation shows that as the aileron deflection is increased to 10 degrees the aircraft enters a spin. The difference between the critical aileron deflection predicted by the continuation method and that shown in the simulation could either be a result of the transient aileron deflection in the simulation or a result of the different aerodynamic curve fits used in the continuation method algorithm and the simulation program.

A recovery from the spin is attempted by reducing the aileron deflection to negative twelve degrees, at which point the steady spin becomes unstable because of a Hopf bifurcation (see Figure 6). The recovery is not successful because a steady oscillatory spin develops. Recall that the rudder is ineffective at angles of attack greater than 55 degrees so only the ailerons and elevator are available to attempt recovery from a spin. The lack of rudder authority at high angles of attack could make it impossible to recover from a developed spin.

Since it is difficult or impossible to recover from a spin in the F-14 it is clearly desirable to stay out of a spin. The saddle-node bifurcations that occur at aileron deflections of positive and negative twelve degrees were responsible for the aircraft going into a spin. If the aileron deflections were limited to values less than those at which these bifurcations occur it might be possible to avoid entering a spin. Figure 8 shows the loci of elevator and aileron deflections at which the saddle-node bifurcations responsible for the spin entry occur. This diagram could be used to put limits on the aileron deflection. Inclusion of a control system could change this figure so the results for an operational F-14 could be different.

Rudder deflection is applied during most lateral maneuvers and would in general change the control surface deflections at which bifurcations occur. Figure 9 shows the steady states of the aircraft as a function of aileron deflection for an elevator deflection of negative 10 degrees and a rudder deflection of negative 2 degrees. The elevator deflection is the same for Figures 6 and 9 so differences in the steady states shown in the two figures are a result of the different rudder deflections.

Applying two degrees of negative rudder deflection has a dramatic effect on the steady states of the aircraft which are at low angles of attack. Figure 6 shows that with no rudder deflection the steady states which are at low angles of attack only exist for aileron deflections between negative 12 and positive

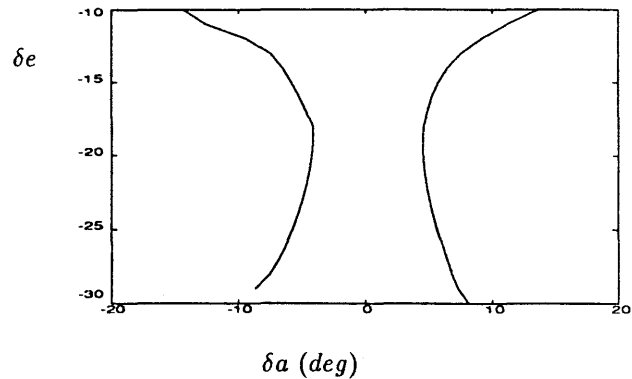


Figure 8: Bifurcation loci for the F-14 for $T = 0$, $\delta r = 0$.

12 degrees. When two degrees of negative rudder are applied (see Figure 9), steady states which are at low angles of attack exist for aileron deflections between negative 10 and positive 30 degrees. Thus, by using the rudder it is possible to apply 18 degrees of extra positive aileron deflection. Note that steady states which have angles of attack greater than 55 degrees are the same for the Figures 6 and 9 because the rudder is ineffective for angles of attack greater than 55 degrees.

Figure 10 shows the combination of aileron and rudder deflections which cause the steady states which are low angles of attack to become unstable. For example, drawing a horizontal line representing zero rudder deflection shows that saddle-node bifurcations cause the steady states which are at low angles of attack to become unstable for aileron deflections larger than positive or negative 12 degrees. Figure 10 could be used to put limits on the aileron deflection for a given rudder deflection, or it could be used to program the aileron and rudder such that that combinations of aileron and rudder deflections at which bifurcations occur could never be realized. Recall that Figure 10 is only valid for an elevator deflection of negative 10 degrees, but similar plots could be made for other elevator deflections.

4.3 Steady Spin Modes

Recall that continuation methods require a known steady state as a starting point for the continuation procedure. It is usually easy to determine steady states which are at low angles of attack, such as the steady states shown in Figure 2. It is a much more difficult task to determine the steady

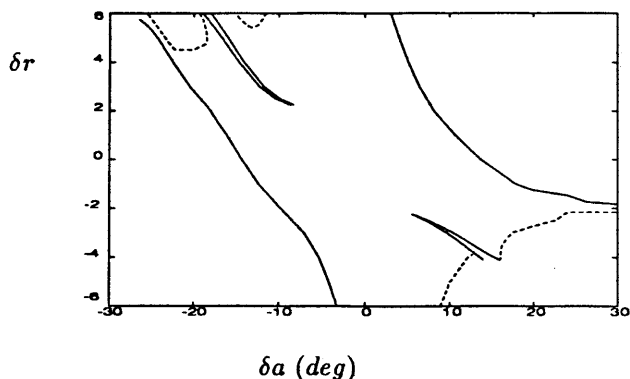


Figure 10: Stability boundary for the F-14 for lateral maneuvers with zero applied thrust and $\delta e = -10$; — saddle-node bifurcation, - - - Hopf Bifurcation.

spin modes of an aircraft and it is usually not possible to be certain that all the steady spin modes of a particular aircraft have been determined.

The approach used to find the spin modes in this work was to guess an initial spin mode as a starting point for the continuation method algorithm; then let the algorithm run until either a true steady spin was determined or the algorithm ran into numerical problems. Spin modes determined by Adams [1972] and Jahnke [1990] for other aircraft were used as a guide for picking the approximate spin modes.

Figure 11 shows the steady spin modes of the F-14 which were found in this work as a function of the elevator deflection. The asymmetry of the aerodynamic model is evident in the spin modes, if the aerodynamic model was symmetric curves 3N and 3P and curves 4N and 4P would be symmetric. Spin modes represented by curves 4N and 4P are flat spins ($\alpha = 90$ degrees) at very high yaw rates. These spin modes were unstable for all control surface deflections used during the course of this work.

Spin modes represented by curves 3N and 3P represent both flat spins ($\alpha = 90$ degrees) and steep spins ($\alpha = 50$ degrees), but only the flat spins are stable. Figure 9 shows that stable steady spins exist for almost the entire range of elevator deflections so it may not be possible to recover from a developed spin with only elevator deflection for zero aileron deflection (Recall that the rudder is ineffective for angles of attack greater than 55 degrees.)

Figure 12 shows an attempted spin recovery with only elevator deflections. A small perturbation in the aileron deflection for an elevator deflection of negative 5 degrees causes the aircraft to enter a spin with a positive roll rate. The elevator deflection is first reduced to negative 20 degrees in an attempt to recover from the spin because the steady spin modes with positive roll rates (3P) are unstable for an elevator deflection of negative 20 degrees (see Figure 11). This attempted recovery is not successful as the aircraft enters an oscillatory spin.

Increasing the elevator deflection to negative 40 degrees, for which no stable or unstable steady spins exist, is also unsuccessful in recovering from the spin. Finally full nose down elevator is applied ($\delta e = -10$ degrees) but this is also unsuccessful in recovery from the spin. This example shows the need to determine the time dependent spin modes along with the steady spin modes in order to develop spin recovery techniques.

V. CONCLUSIONS

The above results show the value of using continuation methods and dynamical systems theory for analyzing the equations of motion for an aircraft. The efficiency of the method makes it possible to analyze complicated aerodynamic models using the complete equations of motion for the entire range of control surface deflections. The results presented here were computed on a micro-VAX and it generally took about one minute to compute curves of steady states such as those shown in Figure 6. Simulations usually took twenty times as long, which shows the efficiency of calculating the steady states with continuation methods.

The method has great potential for designing control laws. Figures like Figure 8 could be used to put limits on the control surface deflections so pilots stay away from jump phenomena. Simple feedback control systems can also be included in the aerodynamic model to determine the effects of control systems on various instabilities. This could be particularly useful for designing control systems for high angle of attack flight where the equations of motion are inherently nonlinear and traditional linear control theory might not be valid.

A knowledge of the control surface deflections which cause bifurcations can also be used to escape from motions caused by a jump in the state of the aircraft. No successful spin recovery technique was determined for this aircraft because of the presence of stable periodic spins. This points to the need to determine which control surface deflections lead to

the existence of stable periodic spins. Continuation methods can be extended to determine periodic motions as a function of the parameters of the system just as the fixed points have been found in this work.

ACKNOWLEDGEMENTS

This work was partly supported by CALTECH funds and partly supported by a grant from the National Aeronautics and Space Administration, Ames Dryden Flight Research Center. The F-14 aerodynamic model was supplied by Joe Gera, Acting Assistant Branch Chief, Vehicle Technical Branch, Ames Dryden Flight Research Center.

REFERENCES

1. Phillips, W. H., "Effect of Steady Rolling on Longitudinal and Directional Stability", NASA TN No. 1627, June 1948.
2. Gates, O. B. and Minka, K., "Note on a Criterion for Severity of Roll-Induced Instability", Journal of the Aero/Space Sciences, May, 1959, pp. 287-290.
3. Young, J. W., Schy, A. A., and Johnson, K. G., "Pseudosteady-State Analysis of Nonlinear Aircraft Maneuvers", NASA TP 1758, 1980.
4. Adams, W. M., "Analytic Prediction of Airplane Equilibrium Spin Characteristics", NASA TN D-6926, November 1972.
5. Tischler, M. B. and Barlow, J. B., "Determination of Spin and Recovery Characteristics of a General Aviation Design", Journal of Aircraft, Vol. 18, No. 4, April 1981, pp. 238-244.
6. Guicheteau, P., "Bifurcation Theory Applied to the Study of Control Losses on Combat Aircraft", AGARD/FMP Symposium on "Combat Aircraft Maneuverability", Florence, October 1981.
7. Planeaux, J. B., "High-Angle-of-Attack Dynamic Behavior of a Model High-Performance Fighter Aircraft", AIAA Atmospheric Flight Mechanics Conference, Minneapolis, August 1988, Paper No. 88-4368.
8. Jahnke, C. C. and Culick, F. E. C., "Application of Dynamical Systems Theory to Nonlinear Aircraft Dynamics", AIAA Atmospheric Flight Mechanics Conference, Minneapolis, August 1988, Paper No. 88-4372.
9. Doedel, E. J. and Kernevez, J. P., "Software for Continuation Problems in Ordinary Differential Equations With Applications", Preprint, CALTECH, 1985.
10. Keller, H. B., "Numerical Solution of Bifurcation and Nonlinear Eigenvalue Problems", in

Applications of Bifurcation Theory (Edited by: P. H. Rabinowitz), New York: Academic Press, 1977.

11. Jahnke, C. C., "Application of Dynamical Systems Theory to Nonlinear Aircraft Dynamics", Ph.D. Thesis, California Institute of Technology, Pasadena, California, January 1990.

APPENDIX A

The following examples show how bifurcations can be found and the effect they have on the response of the system. The saddle-node bifurcation (also called a fold or turning point) is the simplest bifurcation with one zero eigenvalue. Saddle-node bifurcations cause the creation (or destruction) of one stable steady state (node) and one unstable steady state (saddle), hence the name saddle-node bifurcation. Saddle-node bifurcations are common in physical problems and can cause jump phenomena.

The pitchfork bifurcation is also characterized by one zero eigenvalue and the creation or destruction of two steady states, but it is more complicated than the saddle-node bifurcation. Two branches of fixed points intersect at a pitchfork bifurcation, but only one branch of steady states exists at a saddle-node bifurcation. The Hopf bifurcation is the simplest example of a bifurcation for which one pair of complex eigenvalues has zero real parts. Hopf bifurcations are common in physical systems and cause the creation or destruction of periodic motion.

A1. Saddle-Node Bifurcation

Consider the equation

$$\dot{x} = \mu - x^2.$$

The steady states of this equation ($\dot{x} = 0$) are given by $x = \pm\sqrt{\mu}$. Two steady states exist if μ is positive while no steady states exist if μ is negative. Linearizing the equation about the steady state $x = \sqrt{\mu}$ gives the equation

$$\dot{u} = -2\sqrt{\mu}u$$

where $u = x - \sqrt{\mu}$. The eigenvalue, $\lambda = -2\sqrt{\mu}$, is negative so the steady state is stable. Applying the same analysis to the steady state $x = -\sqrt{\mu}$ shows that it is unstable. These results are plotted in Figure 13. Solid lines represent stable steady states and dashed lines represent unstable steady states. The vertical lines with the arrows show the evolution of

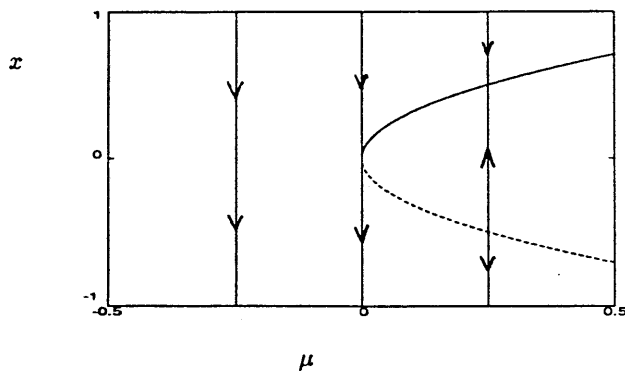


Figure 13: Saddle-node bifurcation.

the system in time for fixed values of μ and some initial condition (x, μ) .

This system has a bifurcation at $\mu = 0$ as the eigenvalue of the linearized system is zero at the steady state $(x, \mu) = (0, 0)$. Thus, the system should exhibit qualitatively different behaviors for μ less than zero and μ greater than zero. This is clearly shown in Figure 14 which shows the time evolution of the system when μ is greater than zero and when μ is less than zero for the same initial value of x . If μ is positive the system approaches the steady state, $x = \sqrt{\mu}$. If μ is negative no stable steady states exist and x continually decreases.

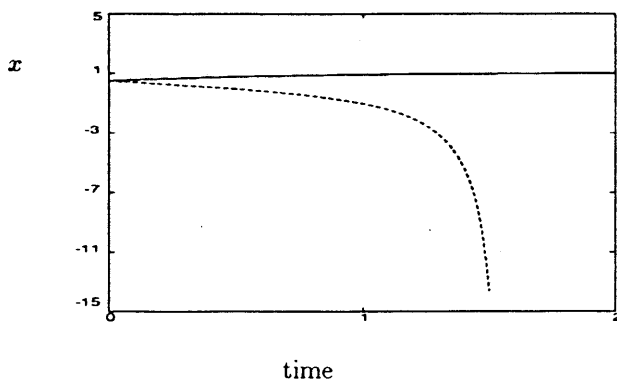


Figure 14: Simulation of saddle-node bifurcation; — $\mu = 1$, - - - $\mu = -1$.

A2. Pitchfork Bifurcation

Consider the equation

$$\dot{x} = x(\mu - x^2).$$

The steady states of this equation are $x = 0, \pm\sqrt{\mu}$. If μ is less than zero one steady state exists, while if μ is greater than zero three steady states exist. Linearizing about the steady state $x = 0$ gives

$$\dot{u} = \mu$$

where $u = x - 0$, so the steady state $x = 0$ is stable when μ is less than zero and unstable when μ is greater than zero. Linearizing about the steady state $x = \sqrt{\mu}$ gives

$$\dot{u} = -2\mu$$

where $u = x - \sqrt{\mu}$, so this steady state is always stable. Note that this steady state only exists for μ greater than zero. Applying this same analysis to the steady state $x = -\sqrt{\mu}$ shows that it is always stable.

These results are shown graphically in Figure 15. This system has a bifurcation at μ equals zero because the eigenvalue of the linearized system at the steady state $(x, \mu) = (0, 0)$ is zero. As μ is increased past zero this bifurcation causes the $x = 0$ steady states to become unstable and two new stable steady states to appear. This equation is symmetric in x so either new steady state could be approached.

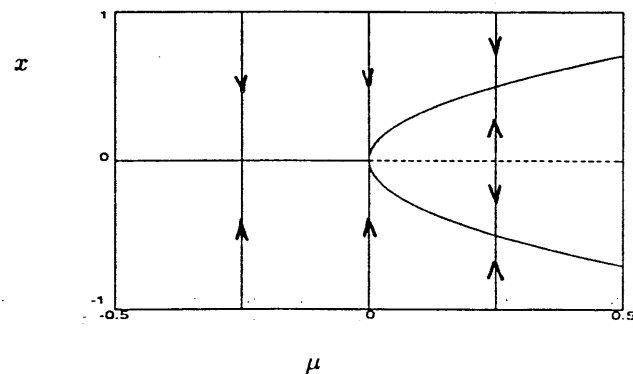


Figure 15: Pitchfork bifurcation.

A3. Hopf Bifurcation

Consider the system written in polar coordinates

$$\begin{aligned} \dot{r} &= r(\mu - r^2), \\ \dot{\theta} &= 1. \end{aligned}$$

This system has a fixed point at the origin for all values of μ and a periodic orbit, or limit cycle, for

$\mu > 0$ given by $r = \sqrt{\mu}$. The system must be transformed into rectangular coordinates to calculate the eigenvalues of the steady state $r = 0$. In rectangular coordinates the system is

$$\begin{aligned}\dot{x} &= \mu x - y - x(x^2 + y^2) \\ \dot{y} &= x + \mu y - y(x^2 + y^2).\end{aligned}$$

Linearizing about the origin we find

$$\begin{pmatrix} \dot{x} \\ \dot{y} \end{pmatrix} = \begin{pmatrix} \mu & -1 \\ 1 & \mu \end{pmatrix} \begin{pmatrix} x \\ y \end{pmatrix}$$

which has eigenvalues $\lambda = \mu \pm i$, where $i = \sqrt{-1}$. The origin is stable for $\mu < 0$ and unstable for $\mu > 0$. For $\mu = 0$ the eigenvalues are purely imaginary. Thus, the origin undergoes a Hopf bifurcation for $\mu = 0$ which creates the limit cycle $r = \sqrt{\mu}$. This is shown in Figure 16.

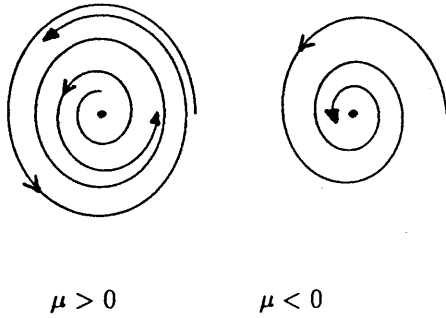


Figure 16: Simulation of Hopf bifurcation.

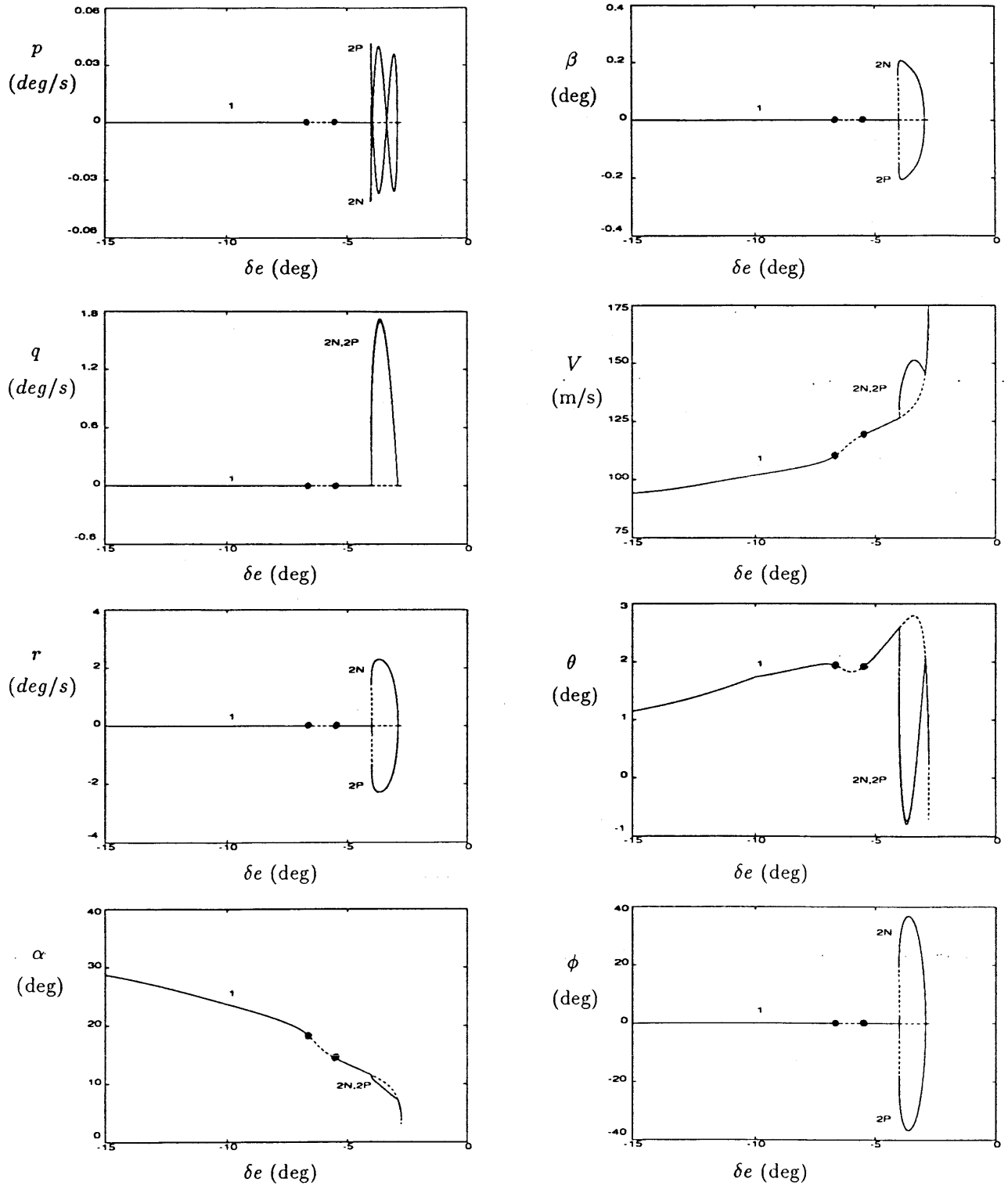


Figure 2: Steady states of the F-14 which are low angles of attack for $\delta a=0$, $\delta r=0$, $T=0$;
 — stable, - - - unstable, • - Hopf bifurcation.

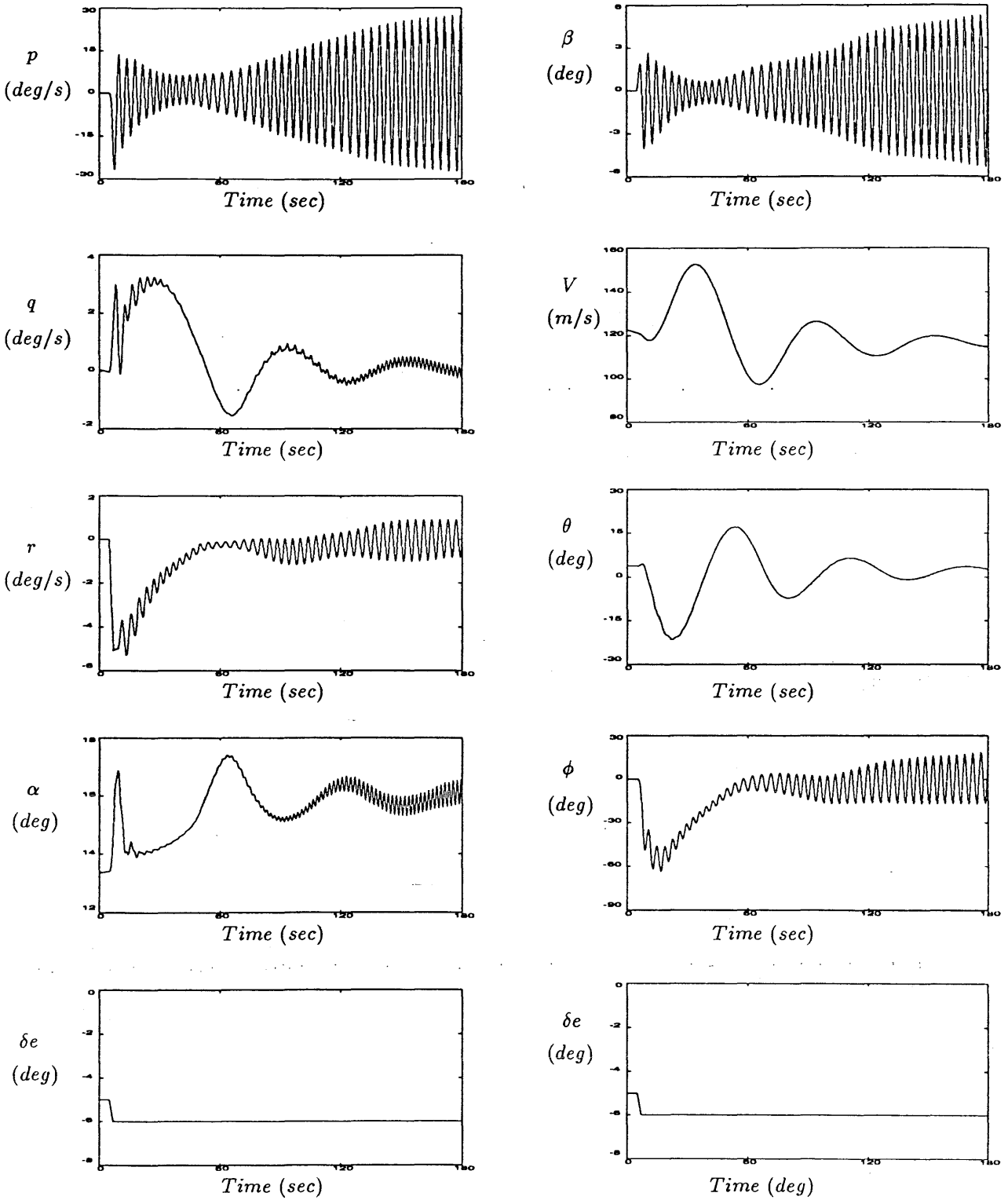


Figure 3: Simulation of wing rock instability for the F-14 with a one-tenth of a degree perturbation in the aileron deflection for times between 5 and 7 seconds, $T=0$, $\delta r=0$.

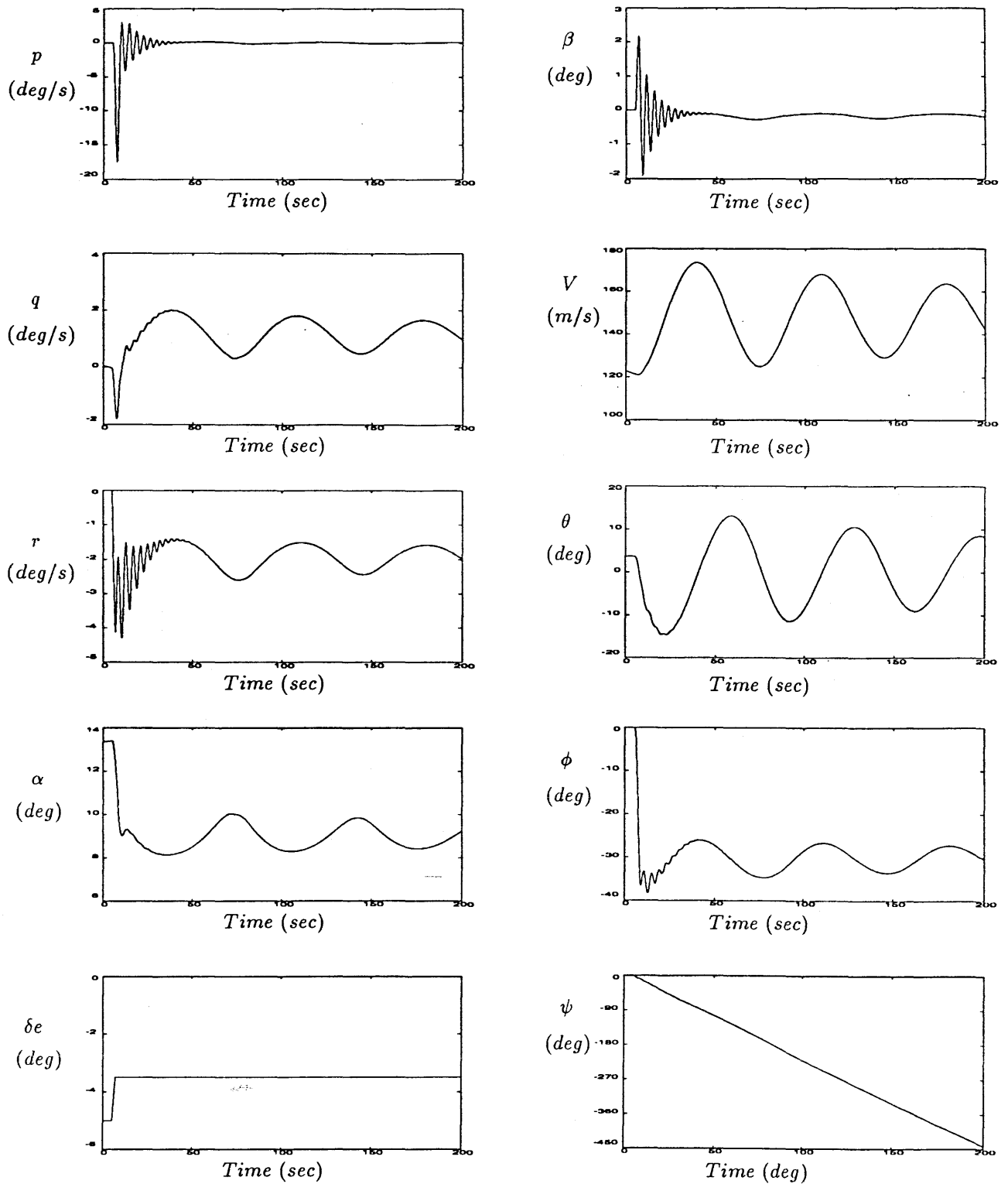


Figure 4: Simulation of spiral divergence instability for the F-14 with a one-tenth of a degree perturbation in the aileron deflection for times between 5 and 7 seconds, $T=0$, $\delta r=0$.

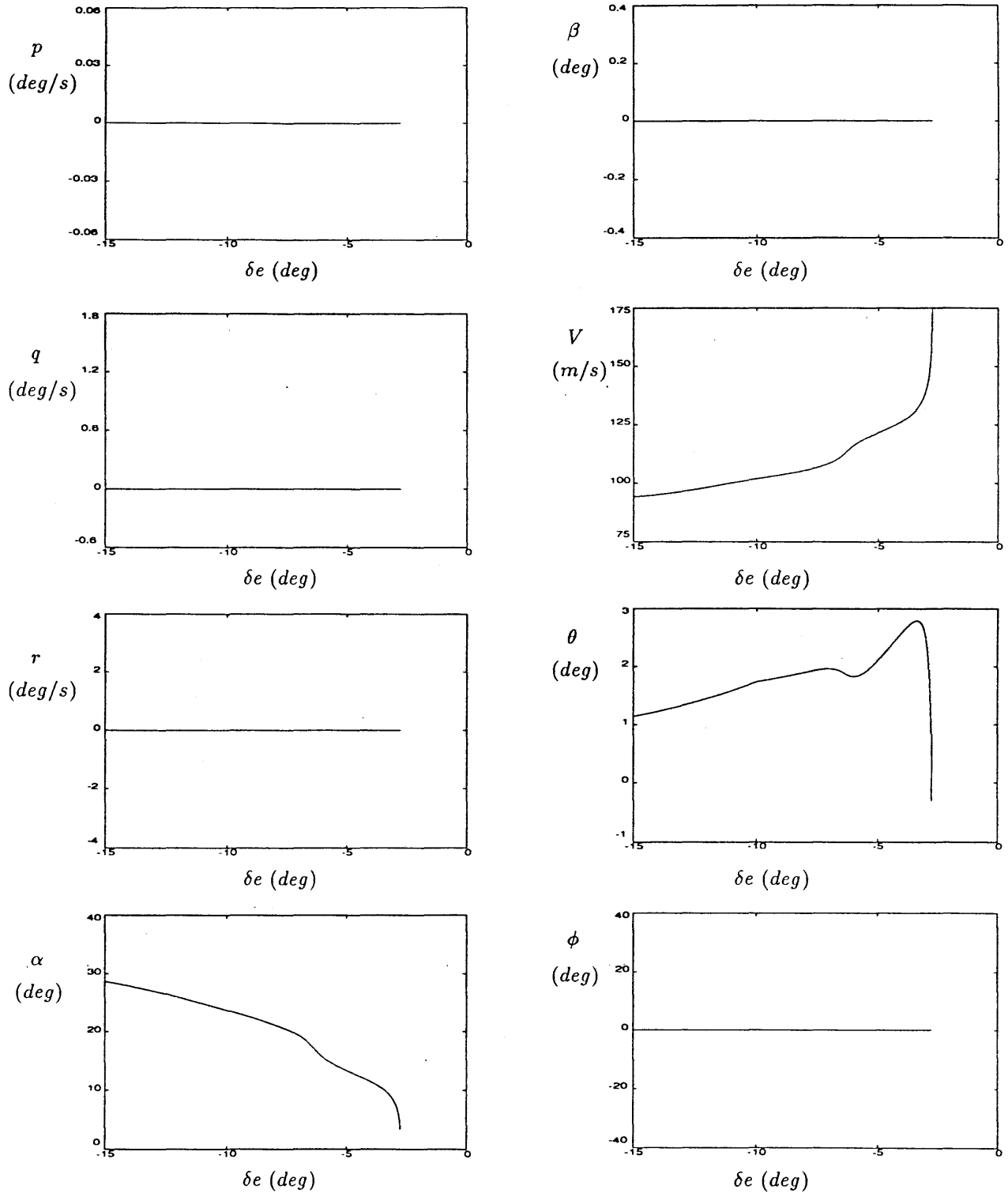


Figure 5: Steady states of the F-14 which are at low angles of attack with sideslip and roll rate feedback to the ailerons, $T=0$, $\delta r=0$, $\delta a = -.1p - .3\beta$; — stable.

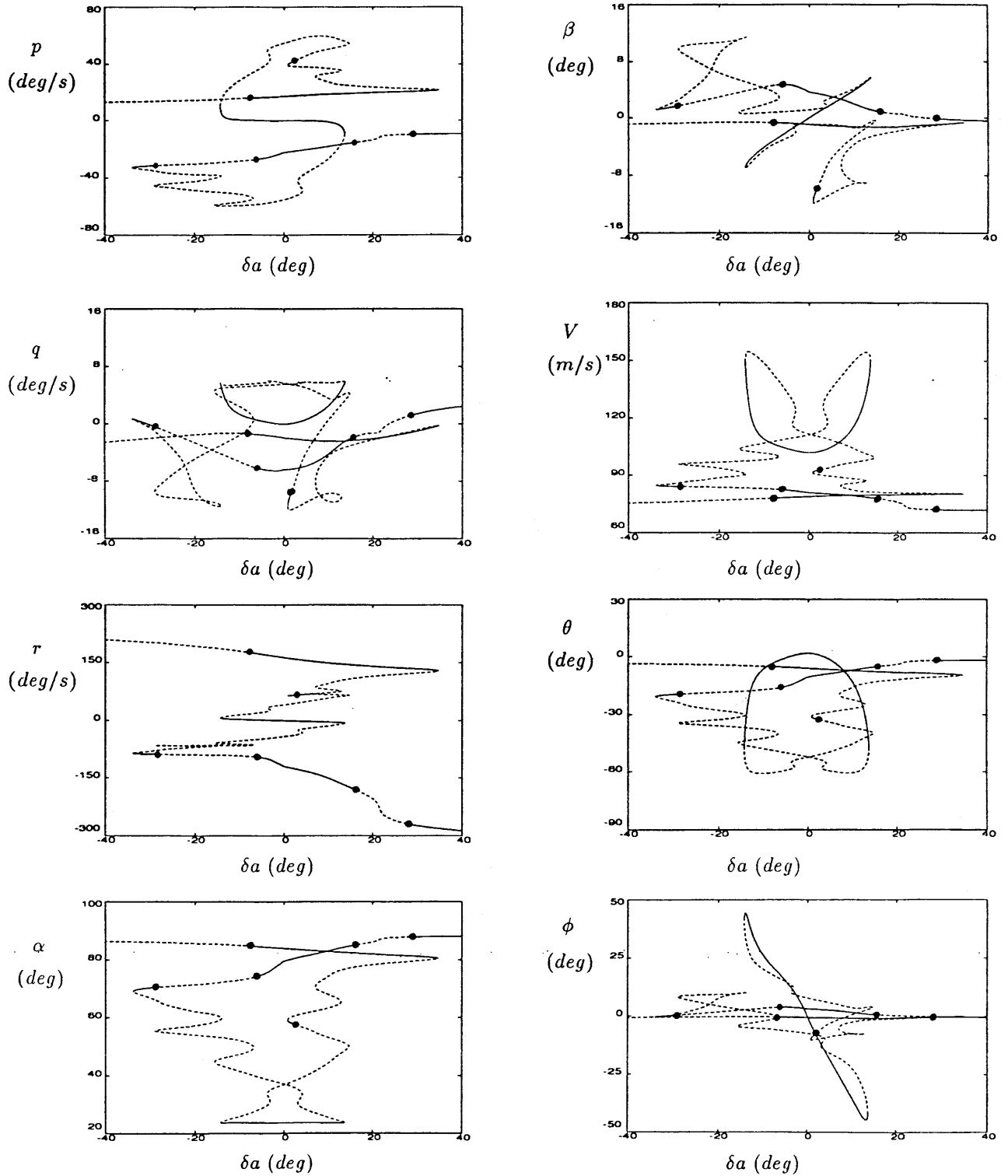


Figure 6: Steady states of the F-14 for lateral maneuvers with $\delta e = -10$, $\delta r = 0$, $T = 0$; — stable, --- unstable, • - Hopf bifurcation.

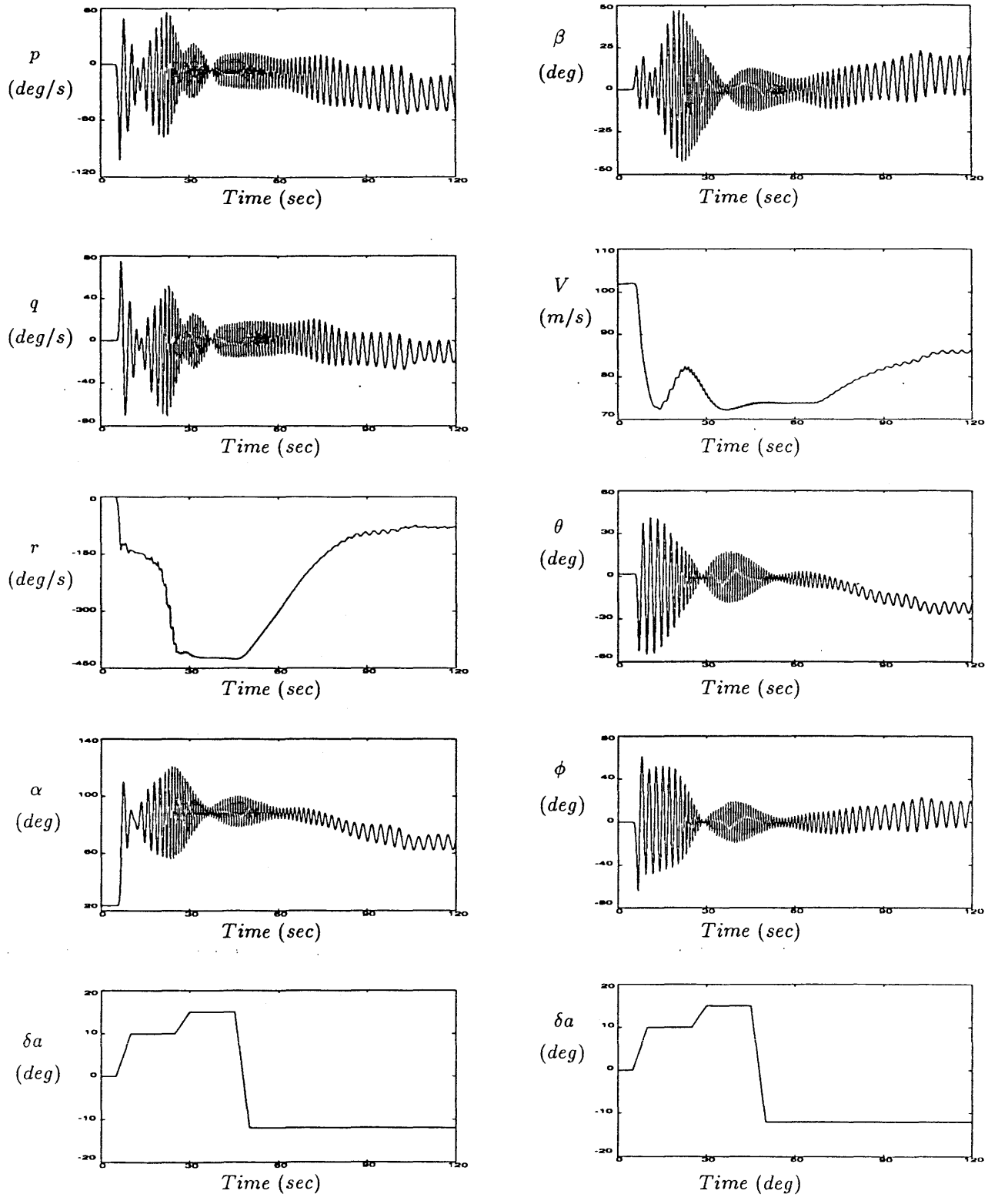


Figure 7: Simulation of instability during a lateral maneuver for the F-14 with $T=0$, $\delta e=-10$, $\delta r=0$.

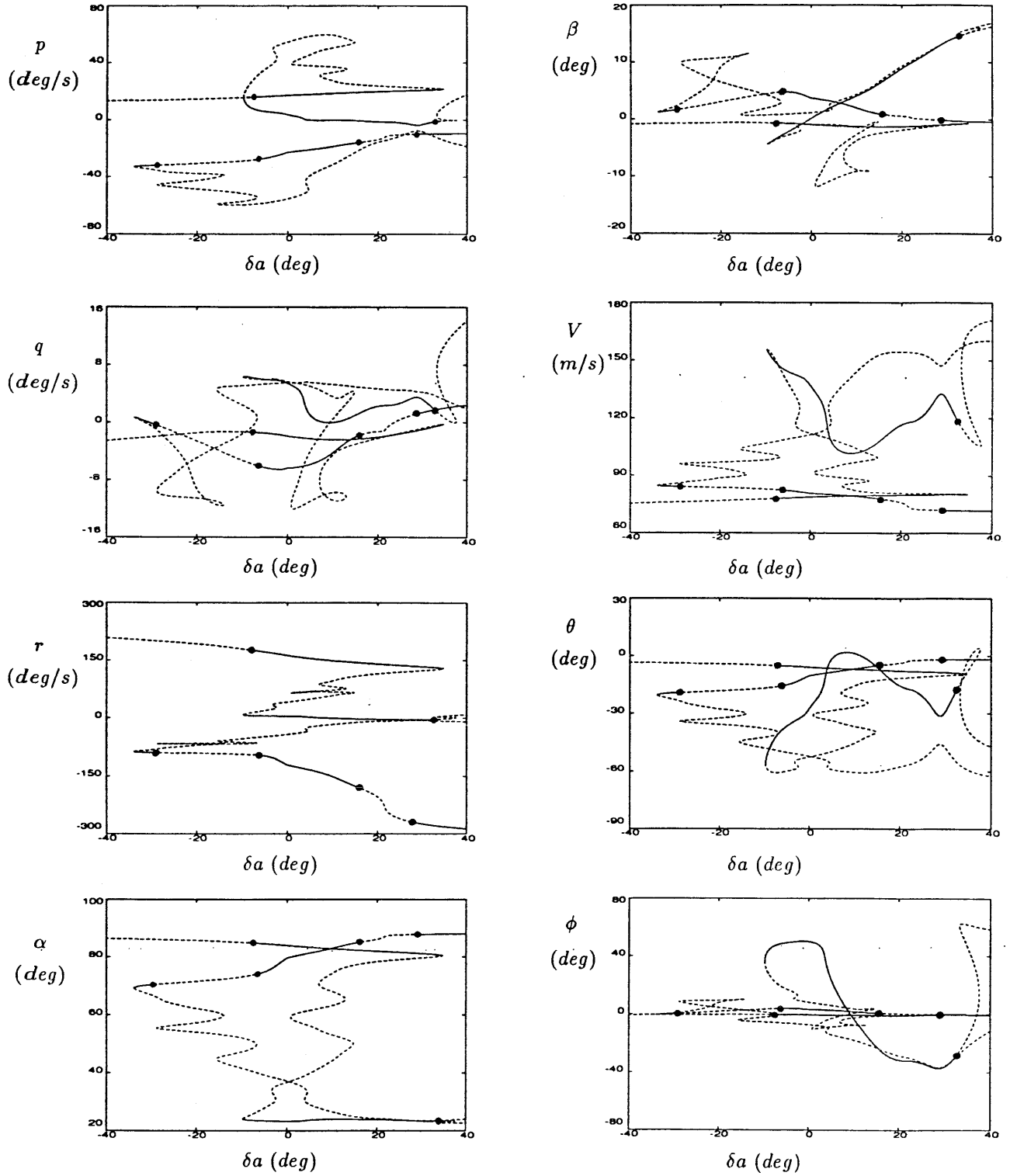


Figure 9: Steady states of the F-14 for lateral maneuvers with $\delta e=-10$, $\delta r=-2$, $T=0$; — stable, - - - unstable, • - Hopf bifurcation.

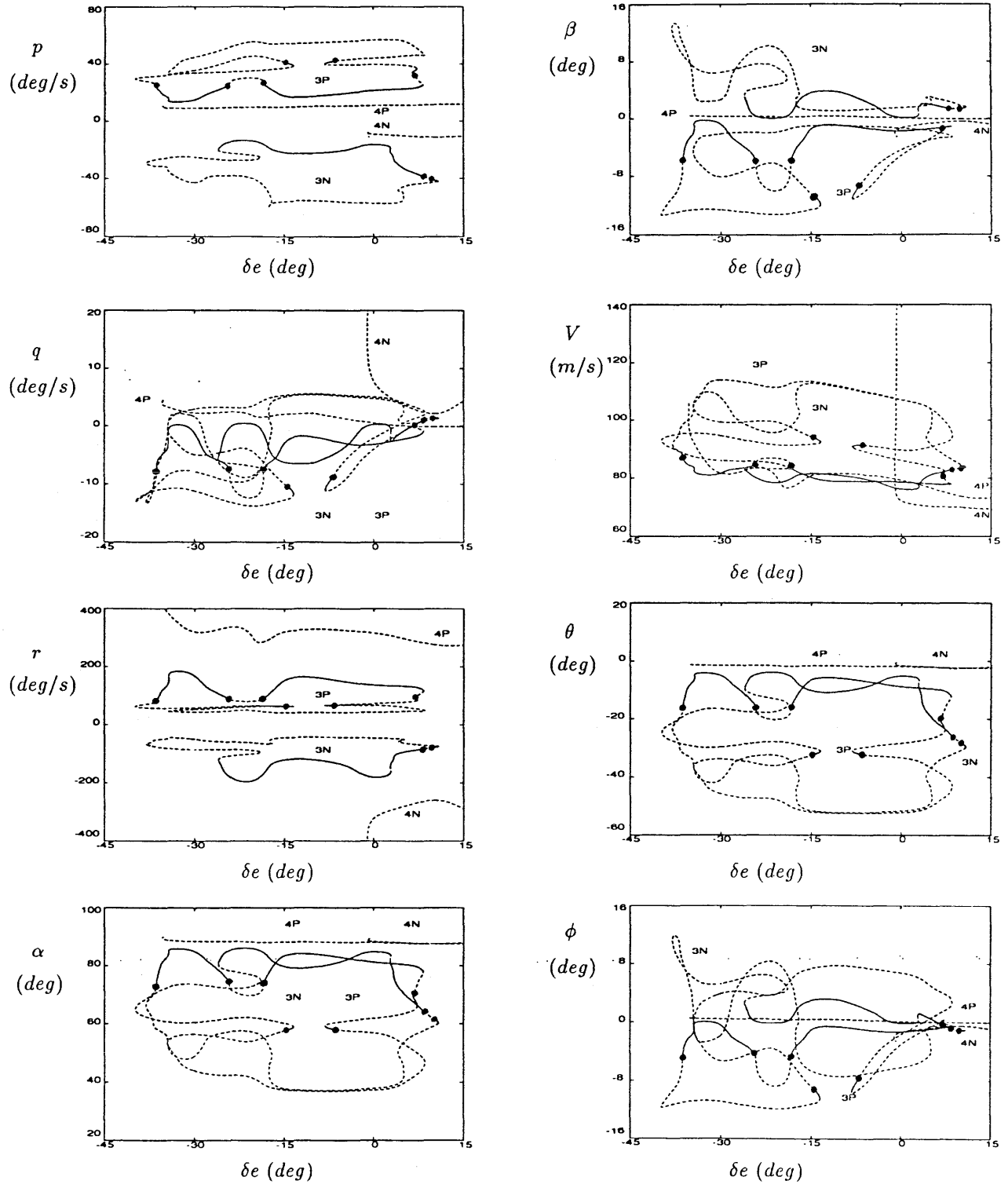


Figure 11: Steady state spin modes of the F-14 for $\delta a=0$, $\delta r=0$, $T=0$; — stable, - - - unstable, • - Hopf bifurcation.

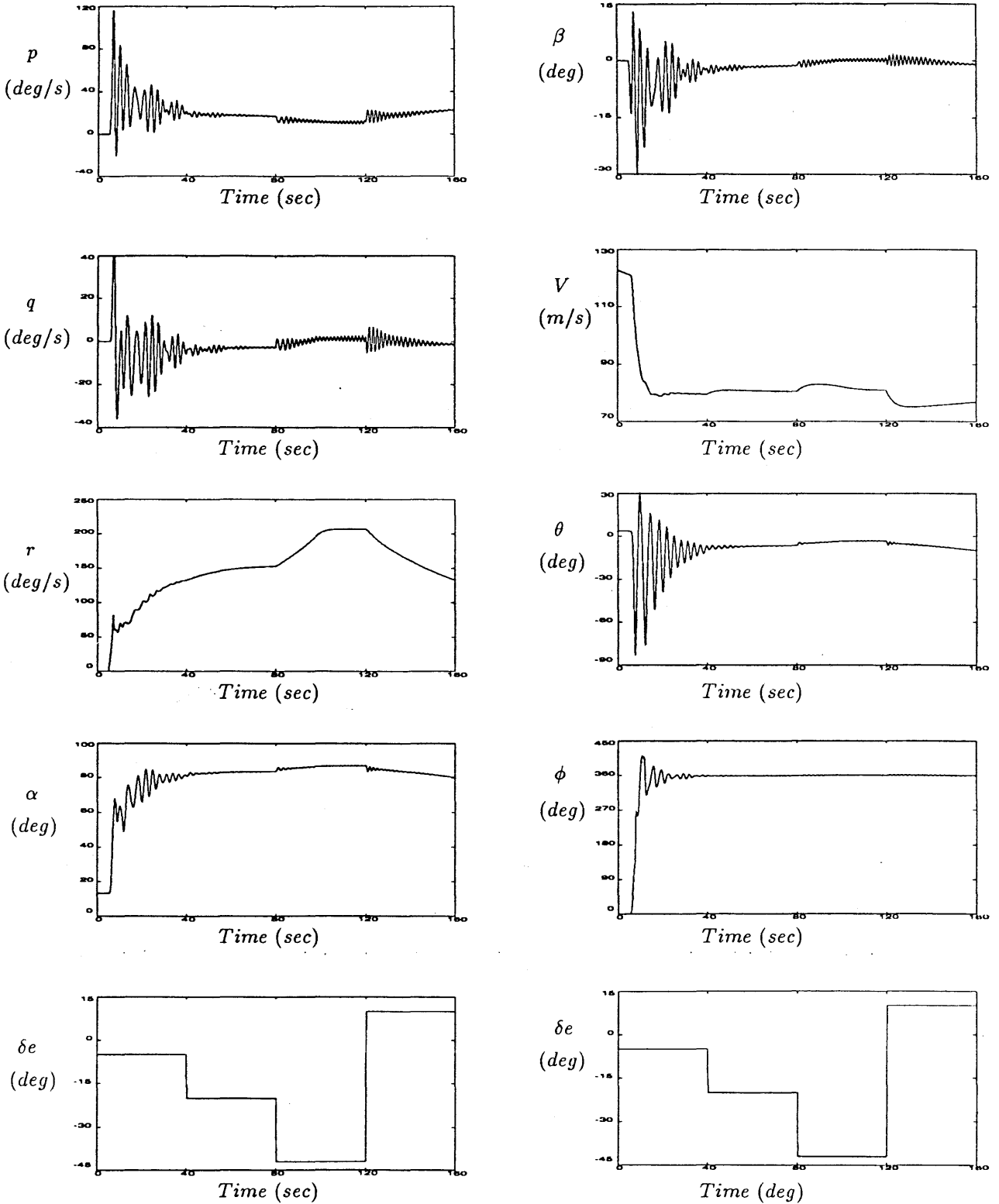


Figure 12: Simulation of a spin entry caused by a one degree aileron perturbation and attempted recovery with ailerons and rudder neutral for zero applied thrust.